Food Hydrocolloids 99 (2020) 105348

Contents lists available at ScienceDirect

Food Hydrocolloids

journal homepage: www.elsevier.com/locate/foodhyd

Exploring *in vitro* gastric digestion of whey protein by time-domain nuclear magnetic resonance and magnetic resonance imaging

Ruoxuan Deng[a,b,*], Anja E.M. Janssen[b], Frank J. Vergeldt[c], Henk Van As[c], Cees de Graaf[a], Monica Mars[a], Paul A.M. Smeets[a,d]

[a] Division of Human Nutrition and Health, Wageningen University & Research, Wageningen, the Netherlands
[b] Laboratory of Food Process Engineering, Wageningen University & Research, Wageningen, the Netherlands
[c] Laboratory of Biophysics, Wageningen University & Research, Wageningen, the Netherlands
[d] Image Sciences Institute, University Medical Center Utrecht Brain Center, Utrecht University, Utrecht, the Netherlands

ARTICLE INFO

Keywords:
Time-domain NMR
MRI
Whey protein
Gel
In vitro
Gastric digestion

ABSTRACT

Gastric digestion is crucial for protein breakdown. Although it has been widely studied with *in vitro* models, verification *in vivo* remains a big challenge. Magnetic resonance imaging (MRI) has the potential to bridge this gap. Our objective was to use the transverse relaxation time (T_2) and rate ($R_2 = T_2^{-1}$) to monitor hydrolysis of protein-rich food during *in vitro* gastric digestion. Whey protein solution and heat-induced hydrogels were digested by means of simulated gastric fluid (SGF). Free amino groups (–NH_2 groups) and protein concentration in the supernatant were measured. T_2 and R_2 of the digestion mixture were determined by time-domain nuclear magnetic resonance (TD-NMR) and MRI. Subsequently, relative amplitudes (TD-NMR) for different T_2 values and T_2 distribution (MRI) were determined. For the solution, protein concentration and T_2 did not change during digestion. For the gels, water in supernatant and gel phase could be discriminated on the basis of their T_2 values. During digestion, R_2 of supernatant correlated positively with protein (–NH_2 groups) concentration in SGF. Also, the decrease in relative amplitude of gel fraction correlated linearly with the increase of supernatant protein concentration. MRI T_2-mapping showed similar associations between R_2 of supernatant and protein (–NH_2 groups) concentration. In conclusion, T_2-measurements by TD-NMR and MRI can be used to monitor *in vitro* gastric digestion of whey protein gels; TD-NMR measurements contributed to interpreting the MRI data. Thus, MRI has high potential for monitoring *in vivo* gastric digestion and this should be further pursued.

1. Introduction

Gastric digestion is a crucial step for the breakdown of protein-rich foods (Singh & Gallier, 2014). Both gastric fluid, consisting of acid and pepsin, and the mechanical movement of the stomach are essential for the digestive process (Bornhorst & Paul Singh, 2014). The kinetics of gastric digestion plays a key role in subsequent physiological processes such as gastric emptying and nutrient absorption. *In vitro* digestion models have been developed as useful tools to investigate digestion (Brodkorb et al., 2019; Kong & Singh, 2008; Minekus et al., 2014). The chemical composition of digesta sampled from these model systems can then be analysed, for example with the OPA (o-phthaldialdehyde) method, sodium dodecyl sulfate–polyacrylamide gel electrophoresis (SDS-PAGE), size-exclusion chromatography and mass spectrometry (Luo, Boom, & Janssen, 2015; MacIerzanka et al., 2012; Nyemb et al., 2016). However, verifying *in vitro* findings *in vivo* (especially in humans) remains a big challenge. Here, we propose that magnetic resonance techniques have the capability to monitor the gastric digestion of protein and can be used to bridge the gap between *in vitro* model systems and *in vivo* digestion.

Time domain nuclear magnetic resonance (TD-NMR) provides information on the state of water proton in foods, and has been widely used as a characterization and process quality control tool in different food systems (van Duynhoven, Voda, Witek, & Van As, 2010). With TD-NMR, the transverse relaxation time (T_2) of water is determined via the transverse relaxation of ^1H protons. T_2 or the relaxation rate R_2 ($R_2 = T_2^{-1}$) of every water pool provides insight into the degree of exchange of either water protons with protein protons or the exchange of water between water pools such as bulk water with the (internal) water fraction in/around the proteins (Kirtil, Cikrikci, McCarthy, & Oztop, 2017; Mariette, 2009; Peters et al., 2016). For instance, an earlier study showed a linear positive association between R_2 and

* Corresponding author. Division of Human Nutrition and Health, Wageningen University & Research, Wageningen, the Netherlands.
E-mail address: ruoxuan.deng@wur.nl (R. Deng).

https://doi.org/10.1016/j.foodhyd.2019.105348
Received 21 July 2019; Received in revised form 23 August 2019; Accepted 28 August 2019
Available online 29 August 2019

casein concentration in solution (Le Dean, Mariette, & Marin, 2004). Different proton populations (e.g. having different chemical exchange and/or different mobility due to the local environment) arise at different T_2 values, and therefore can be used to discriminate different water fractions in the whole system (Bosmans et al., 2012; Munialo et al., 2016). Thus, the variation in T_2 (or R_2) and the corresponding proton population can be used to indicate the change of macromolecule concentration, water migration, structure in food matrices (Peters et al., 2016). As these above-mentioned changes also take place during digestion, we hypothesize that *in vitro* gastric digestion processes can be monitored by TD-NMR. Bordoni et al. (2014, 2011) investigated *in vitro* digestion using TD-NMR, and found it can detect accessibility of digestion juice to the food matrix during digestion. Therefore, it is worthwhile to further explore other possibilities of TD-NMR to quantify the hydrolysis of protein during digestion.

Magnetic resonance imaging (MRI) is a non-invasive technique that, among numerous other applications, can be used to examine gastric emptying *in vivo*. MRI can not only provide information on the volume of the gastric content and gastric emptying, but also on intra-gastric air, phase separation and clot formation (Marciani, 2011; Spiller & Marciani, 2019). An earlier study showed that the viscosity of locust bean gum meal is linearly associated with R_2 *in vitro* ($R^2 = 0.99$), and highlighted the possibility to monitor changes in meal viscosity in the gastric lumen *in vivo* by measurement of T_2 (Marciani et al., 1998). However, to our knowledge, the potential of T_2 mapping by MRI for monitoring the hydrolysis of nutrients during gastric digestion has not been further explored. Likewise, MRI has also been applied for visualizing the food state spatially (i.e. water content, fat content, molecular migration, structure change) *in vitro* (Collewet et al., 2013; Lavenson, Tozzi, McCarthy, Powell, & Jeoh, 2011; Li, Li, & Zhang, 2018; Nott & Hall, 2005). Because they share similar relaxation principles, T_2 measurements by MRI can be validated with TD-NMR experiments, which can provide extra information on the relaxation parameters (Mariette, 2009). Compared with TD-NMR, T_2-mapping by MRI holds the advantage of visualizing T_2 spatially and the possibility to study digestion *in vivo* in humans. Therefore, we explore if T_2-mapping is a useful method to investigate *in vitro* gastric digestion of protein and bridge the gap between *in vitro* and *in vivo* studies.

The objective of this study was to use T_2 measurements by TD-NMR and MRI to monitor protein hydrolysis during *in vitro* gastric digestion, so as to lay a foundation for further *in vivo* studies. We used whey protein solution and heat-induced whey protein hydrogels since these are widely used as liquid and solid protein-rich model foods (MacIerzanka et al., 2012; Nyemb et al., 2016; Nyemb-Diop et al., 2016; Singh, Ye, & Ferrua, 2015). First, the digestion process was monitored by quantifying free amino groups (-NH_2 groups) and protein concentration in digestion supernatant during *in vitro* gastric digestion; Second, T_2 and R_2 were measured during *in vitro* gastric digestion with the use of TD-NMR and MRI; Third, the associations between R_2 (TD-NMR) and protein hydrolysis was examined; Finally, MRI T_2 measurements were used to investigate the feasibility of monitoring protein gel digestion.

2. Materials and methods

2.1. Materials

Pepsin from porcine gastric mucosa (3412 activity units/mg) and all other chemicals were purchased from Sigma Aldrich, Inc. (St. Louis, USA). Whey Protein Isolate (WPI) was purchased from Davisco Food International, Inc. (Le Sueur, USA), with protein content of 97.9 g/100 g dry solid. Milli-Q water (resistivity 18.2 MΩcm at 25 °C, Merck Millipore, Billerica, USA) was used in all experiments.

2.2. Preparation of protein solution and gel

WPI solution and gel were prepared as described by Luo et al. (2015). WPI was dissolved in water (15 wt% or 20 wt%) and stirred at room temperature for at least 2 h. The protein solutions were used within one day. To prepare the gels, the solutions were centrifuged at 1000 rpm for 10 min to eliminate air bubbles, and were poured into Teflon tubes and then heated in a 90 °C water bath for 30 min. After that, the Teflon tubes were immediately cooled in an ice-water bath. The gels were stored within the Teflon tubes at 4 °C, 1–5 days prior to use. The gels were grinded into 30.0 ± 5.0 mg particles before the digestion.

2.3. Preparation of simulated gastric fluid

Phosphate buffer (Na_2HPO_4–H_3PO_4–NaCl buffer, pH 2.0, I = 154 mM) was used as the simulated gastric fluid (SGF), and pepsin was added to achieve activity at 2000 activity units/mL in the final mixture, as recommended by Minekus et al. (2014) and Brodkorb et al. (2019). For the control group, no pepsin was added to the SGF.

2.4. Time domain NMR

To prepare for the TD-NMR tests, 30 μL WPI solution or 30.0 mg gel was mixed with 120 μL SGF in 7-mm NMR tubes that were afterwards sealed to prevent water loss during the experiment. After mixing, the tubes were kept in an Eppendorf thermomixer (Eppendorf AG, Hamburg, Germany) at 37 °C and with shaking speed at 300 rpm and timing was started. At time 0, 10, 20, 30, 45, 60, 90 and 120 min, the tubes were moved from the thermomixer to a Maran Ultra NMR spectrometer (Resonance Instruments Ltd., Witney, UK) to perform ^{1}H TD-NMR relaxometry at 0.72 T magnetic field strength (30.7 MHz ^{1}H resonance frequency).

The measurements were controlled by RINMR software (Resonance Instruments Ltd., Witney, UK). The decay of the transverse magnetization, a process characterized by the transverse relaxation time T_2, was measured by the Carr-Purcell-Meiboom-Gill (CPMG) sequence. During the CPMG pulse train, 12288 echoes (five data points per echo) were recorded with an echo time of 1.2 ms. 8 transients were recorded with phase cycling, with a repetition time of 8 s. Each echo in the CPMG echo train was phase corrected and each echo was averaged to one data point using the IDL package (ITT Visual Information Solutions, Boulder, CO, USA). The transverse magnetization decay curves were analysed with a numerical inverse Laplace transform by CONTIN, resulting in a distribution of amplitude at different transverse relaxation times (T_2) (Provencher & Vogel, 1983). From the distribution curve, average T_2 and R_2 values of different components were acquired. For the gel samples, amplitude of gel peak was calculated by the sum of amplitude at every specific T_2 value within the gel peak; the relative amplitude of gel (Rel.Ampl.$_{Gel}$) was calculated by dividing amplitude of the gel peak by the total amplitude in the whole distribution curve. Change of Rel.Ampl.$_{Gel}$ was obtained by dividing the Rel.Ampl.Gel (time t) by Rel.Ampl.Gel (time 0). ΔRel.Ampl.$_{Gel}$ was calculated by subtracting change of Rel.Ampl.$_{Gel}$ in the control condition from that in the digestion condition at the same time point.

2.5. MRI scans during in vitro digestion

For the MRI scans, 5 g of WPI gel particles was mixed with 20 mL SGF in a tube (d = 3.5 mm) that was sealed to prevent water loss during the tests. In one batch, there were 12 tubes which contained triplicates of 4-types sample: 20% gel with SGF with/without pepsin and 15% gel with SGF with/without pepsin. After mixing, the batch of tubes was placed in a 3T MRI scanner (Siemens Magnetom Verio, Erlangen, Germany) and T_2 was measured at time 0 min with a 2D multi-echo spin echo (SE) sequence (repetition time (TR) = 400 m s, 10 echo times

ranging from 13.2 to 132 m s with an echo-spacing of 13.2 m s, matrix = 192*95 mm, FOV = 400*283 mm, in-plane resolution = 2.1 mm, 5.0 mm slice thickness, total acquisition time 18.9 s suitable for breath holding) using a body coil enable future validation *in vivo*. After the scan, the tubes were placed in a water bath shaker at 37 °C, 150 rpm and timing was started. At time 10, 30, 45, 60, 90, 115 min, the tubes were transferred into the MRI scanner to repeat the T_2 measurement.

For each time point T_2 maps were calculated from the images of the ten echo times with the MRmap software which uses a Levenberg -Marquard two-parameter curve fitting (Messroghli et al., 2010). Subsequently, for each tube the T_2 maps were segmented manually with MIPAV software (Bazin et al., 2007), and the distribution of T_2 values was visualized in histogram; besides, the SGF and gel phase were segmented separated as illustrated in Supplemental Fig. 1, and the average T_2 and R_2 of the SGF phase voxels was calculated. The fraction of the gel phase ($Fraction_{Gel}$) was calculated by dividing the number of voxels in the gel phase by the total numbers of voxels in the digestion mixture. The change in $Fraction_{Gel}$ was obtained by dividing $Fraction_{Gel}$ (time t) by $Fraction_{Gel}$ (time 0). The $\Delta Fraction_{Gel}$ was calculated by subtracting the change of $Fraction_{Gel}$ in the control condition from that in the digestion condition.

2.6. In vitro gastric digestion

To measure protein hydrolysis, the amount of free amino groups and the protein concentration in supernatant were measured. The *in vitro* gastric digestion was performed under the same conditions as the TD-NMR measurements. At time 0, 10, 20, 30, 45, 60, 90, 120 min, the supernatant was withdrawn and heated by a pre-heated Eppendorf thermomixer at 90 °C, 850 rpm for 5 min to deactivate pepsin.

2.6.1. Determination of free amino groups

The OPA method as described by Luo et al. (2015) was applied. First, 3.81 g Borax and 100 mg SDS were added to 80 mL Milli-Q water. After these reagents were completely dissolved, 80 mg o-Phthaldialdehyde was dissolved in 2 mL ethanol and added to the above-mentioned solution. Next, 88 mg of DL-dithiothreitol was added and further mixed. Finally, the solution was filled up to 100 mL with Milli-Q water and filtered using a 0.45 mm syringe filter. The solution was kept in the dark. A DU 720 spectrophotometer (Beckman Coulter Inc., Pasadena, USA) was set at 340 nm blanked with 1.5 mL OPA reagent and 0.2 mL Milli-Q water.

To make a calibration curve, 200 μL of 50 mg/L, 100 mg/L, 150 mg/L and 200 mg/L L-serine standard solutions were added to 1.5 mL OPA reagent in a cuvette, and mixed by pipetting for 5 s. The mixtures were measured with the spectrophotometer after standing for 3 min. The same procedure was applied to samples from the digestion experiments.

2.6.2. Protein concentration in supernatant

The protein concentration (the sum of all protein fractions with different sizes) in supernatant was measured with a Bicinchoninic Acid (BCA) kit (Sigma Aldrich, Inc). For the calibration curve, 100 μL of 200 μg/mL, 400 μg/mL, 600 μg/mL, 800 μg/mL and 1000 μg/mL bovine serum albumin (BSA) standard solutions were added to 2 mL BCA reagent and incubated at 37 °C for 30 min. After cooling down to room temperature, the mixtures were transferred into a cuvette and measured at 562 nm in a spectrophotometer (DU 720). The same procedure was applied to samples from the digestion experiments.

2.7. Swelling property of gel

To measure the swelling property of the gels, gel slices with a thickness of 5 mm were soaked in 30 mL SGF without pepsin. At time points 15, 30, 60, 120 min, the gel slices were taken out of the SGF and dried with tissue paper to remove excess liquid, and then weighed. The swelling ratio was calculated as:

$$Swelling\ ratio\ (\%) = \frac{m_t - m_0}{m_0} \times 100\% \quad (1)$$

where m_t represents the weight of the gel at time t and m_0 is the initial weight of the gel.

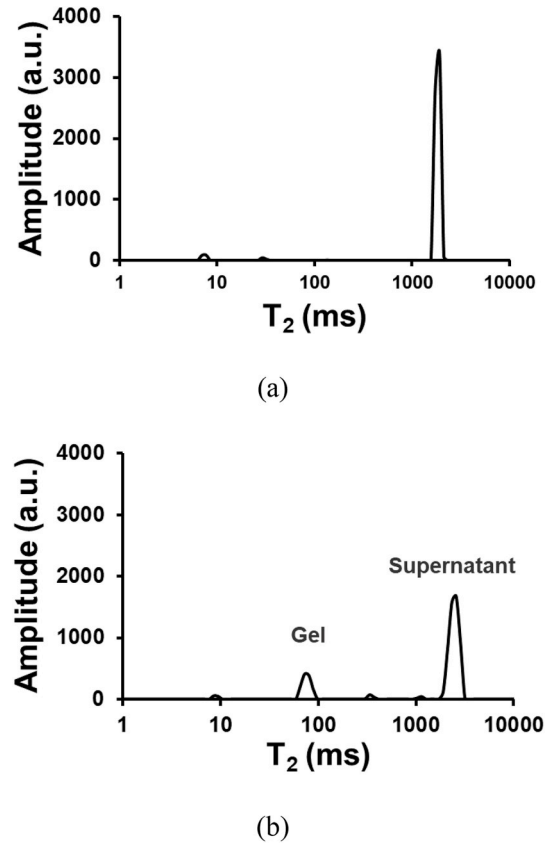

Fig. 1. The T_2 (TD-NMR) distribution of 20% WPI solution (a) and 15% WPI gel (b) with SGF at digestion time 0 min.

3. Results and discussion

3.1. NMR relaxometry of WPI solution or gel

NMR relaxometry was used to measure the T_2 distribution of the WPI solution or the WPI gel (Fig. 1). Due to differences in mobility, local environment and chemical exchange, different proton populations arise at different T_2 values (Peters et al., 2016). This results in the different peaks in the T_2 distribution curve. Thus, the peaks are thought to reflect different components in the digestion mixture. Fig. 1a shows that the major population has a T_2 value around 1700 m s. Since protein solution was mixed with SGF, this major peak represents water protons of the whole mixture (including protein solution and SGF). This value is smaller than the T_2 value of free water, which is 2000–3000 m s, because of the fast proton exchange with protein components (Hills, Takacs, & Belton, 1990). The peak at 7–8 ms might be an fitting error or represent the protein-bound protons, as also observed by Dekkers et al. (2016).

Fig. 1b shows the T_2 distribution of 15% WPI gel with SGF before digestion. Similar to the WPI solution of Fig. 1a, the peak of shortest T_2 at 8 ms represents the protein-bound proton population; the peak of longest T_2 at 2400 ms represents the water proton population in the supernatant phase, labelled with Supernatant. In contrast to Fig. 1a,

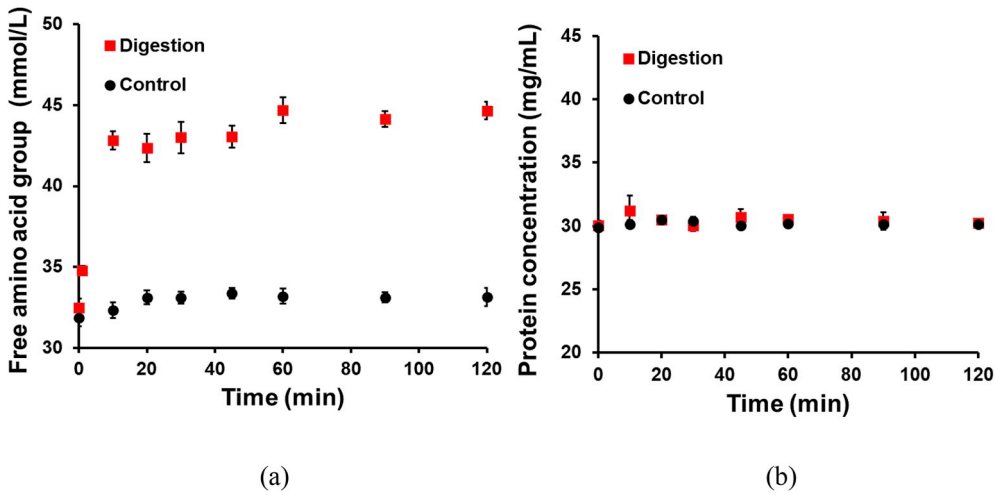

Fig. 2. Free amino groups (a) and protein concentration (b) during an *in vitro* gastric digestion experiment using 20% WPI solution. The control group is without pepsin. Error bars are based on the standard deviation of two or three experiments.

there is one component with an average T_2 of 76 ms. This component represents the water protons located in the protein gel, labelled as Gel. The ratio between the amplitudes of peak Gel and peak Supernatant is around 0.22 which is comparable with the water content ratio (0.21) of protein gel and supernatant. Therefore, further discussion on TD-NMR in this paper will be focused on peak Gel and peak Supernatant to understand the change in both gel phase and supernatant phase during *in vitro* digestion.

We hypothesized that during digestion the average T_2 of supernatant (NMR) would decrease if more protein fraction is released into the digestion mixture. In our digestion system with gels, the relative amplitude of both peak Gel and peak Supernatant would change (e.g. decrease in peak Gel) due to the breakdown of the gels.

3.2. In vitro digestion of WPI solution by NMR relaxometry

Fig. 2a shows the concentration of free amino groups (-NH_2 groups) in the digestion mixture, to quantify the digestion of WPI solution. The concentration of –NH_2 groups increased sharply under digestion conditions, while the concentration in the control condition remained low. This confirms that digestion took place. The protein concentration remained constant over time under both the control and digestion conditions (Fig. 2b). The TD-NMR measurements of the 20% WPI solution are shown in Fig. 3. Under digestive conditions there was no statistically significant change ($p = 0.23$, *t*-test) in the T_2 distribution during *in vitro* digestion (Fig. 3a). In contrast, in the control condition there was a significant decrease ($p < 0.05$, *t*-test) in average T_2 from 1837 ± 69 m s (Mean ± Standard deviation) at 0 min to 1376 ± 134 ms at 120 min (Fig. 3b). The reason for this might be the decrease of the proton mobility which is caused by protein solubility change induced by acidification in the control condition. Acidification and solubility change also take place during digestion, however, due to the action of pepsin, their effects are compensated by the enhanced solubility of proteins and peptides (Dinakar & Kilara, 1996).

After 120 min digestion, the degree of hydrolysis (DH) of whey protein solution was around 3.5%. This confirms that native whey protein is the most resistant protein to peptic hydrolysis (Schmidt, Meijer, Slangen, & Van Beresteijn, 1995). Besides, the protein concentration remained the same during digestion. This might be the reason that the T_2 or R_2 ($=T_2^{-1}$) remained unchanged during digestion. Overall, these results indicate that the T_2 values acquired with NMR do not reflect WPI solution hydrolysis during *in vitro* gastric digestion.

3.3. In vitro digestion of WPI gel and NMR relaxometry

To study the digestion of structured model foods, 15% WPI gel and 20% WPI gel were used. Protein hydrolysis was quantified by measuring the concentration of –NH_2 groups in supernatant over time (Fig. 4a). In agreement with previous studies, 15% gel was digested faster than 20% gel, which is due to the summed effect of diffusion limitation, hydrolysis rate and microstructure transformation (Luo, Borst, Westphal, Boom, & Janssen, 2017). The protein concentration in supernatant (Fig. 4b) was in line with the concentration of –NH_2 groups

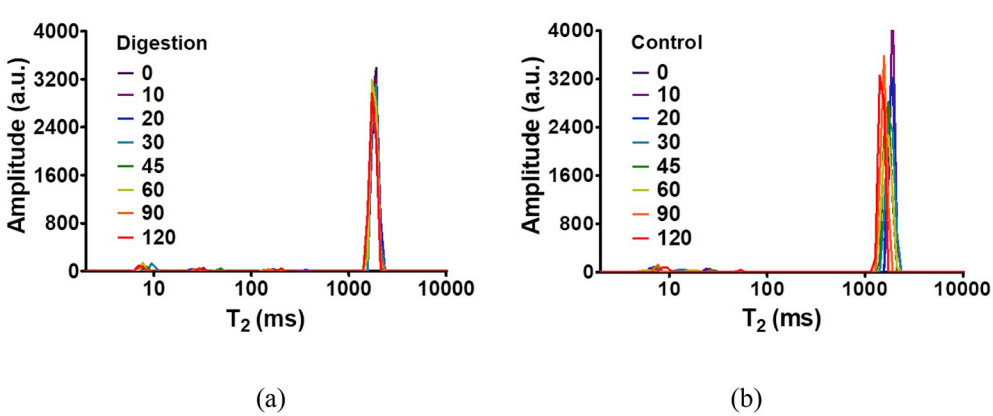

Fig. 3. The T_2 (TD-NMR) distribution of 20% WPI solution under digestion condition (a) and control condition (without pepsin) (b). Curves with colors from black to red represents time points from 0 to 120 min. (For interpretation of the references to color in this figure legend, the reader is referred to the Web version of this article.)

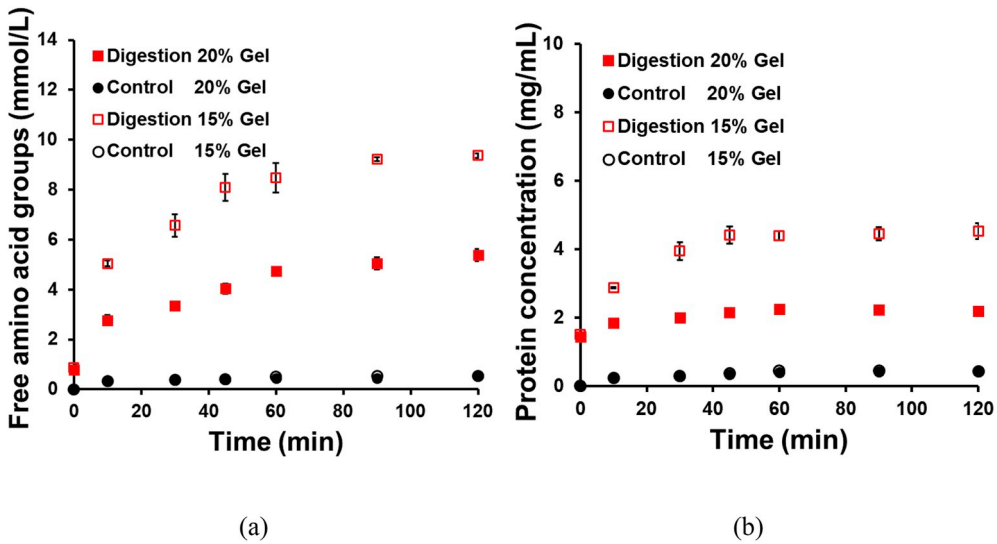

Fig. 4. Free amino groups (a) and protein concentration (b) in supernatant of 20% and 15% WPI gel during *in vitro* gastric digestion. The control groups are without pepsin. Error bars are based on the standard deviation of two or three experiments.

during *in vitro* gastric digestion: positive linear correlations ($R^2 = 0.97$ for 15% WPI gel and $R^2 = 0.94$ for 20% WPI gel) was found (not shown in the figure). After 120 min of digestion, the DH in the supernatant of 15% and 20% was around 23.5%; this indicates that the protein fraction released in the supernatant was highly hydrolysed.

Fig. 5 shows distributed T_2 (TD-NMR) relaxation times of the digestion mixture of 15% gel and 20% gel during *in vitro* digestion. Under digestion conditions, the peak SGF shifted towards shorter T_2 values (Fig. 5a), while there was no significant change of the peak Supernatant under control conditions (Fig. 5b). Over the course of digestion, more protein fraction (-NH_2 groups) are transported from the gel particle into the supernatant, increasing fast proton exchange which

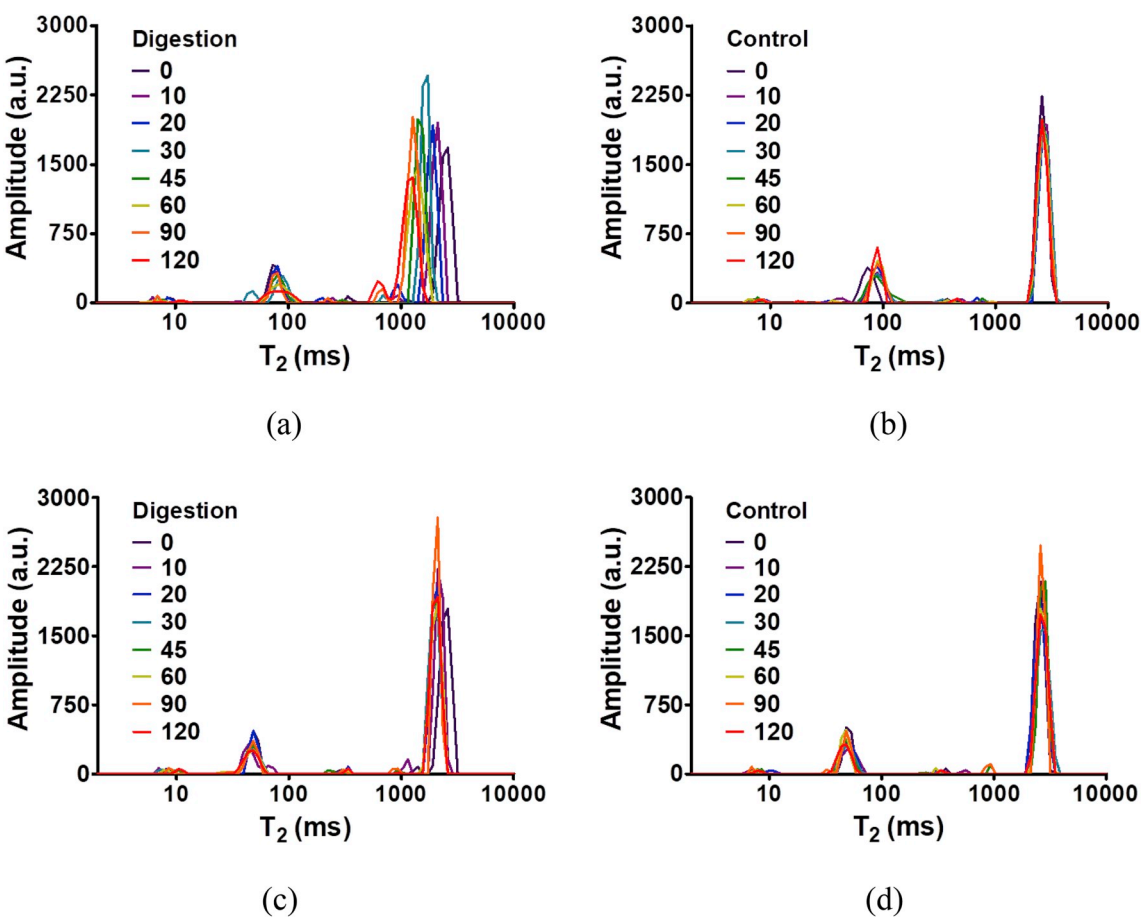

Fig. 5. The T_2 (TD-NMR) distribution of 15% WPI gel under digestion condition (a) and control condition (without pepsin) (b) and that of 20% WPI gel under digestion condition (c) and control condition (d) over time. Curves with colors from black to red represent time points from 0 to 120 min. (For interpretation of the references to color in this figure legend, the reader is referred to the Web version of this article.)

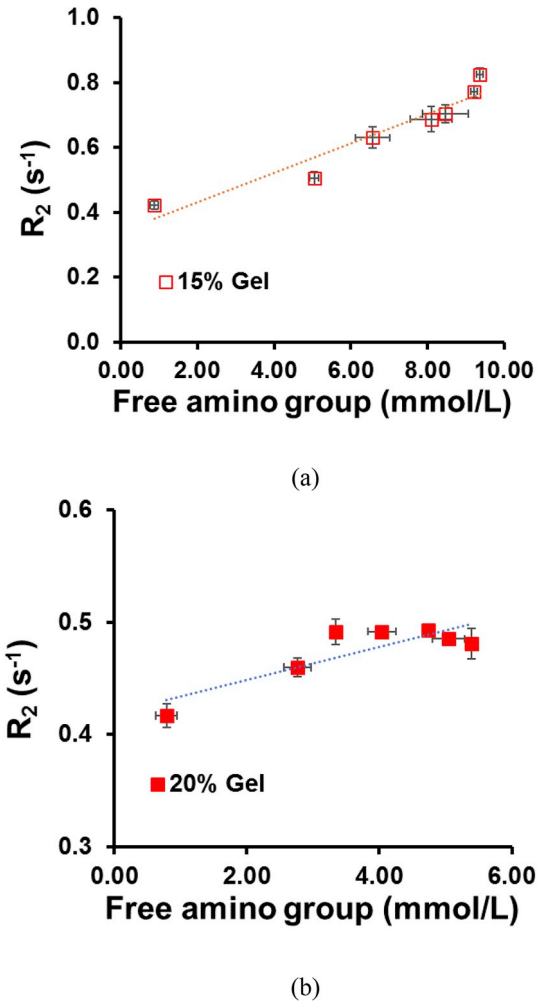

Fig. 6. Correlation between concentration of free amino groups with average R_2 of supernatant of 15% WPI gel (a, $R^2 = 0.91$) and 20% WPI gel (b, $R^2 = 0.71$) during *in vitro* gastric digestion. Error bars are based on the standard deviation of two or three experiments.

results in decreased T_2 of bulk water (water in supernatant). A larger decrease in T_2-supernatant was observed in 15% compared with 20% gel, which is consistent with the faster digestion of 15% gel. Based on the study by Le Dean et al. (2004), a linear relation between R_2 and protein concentration is expected. Since in this case the concentration of $–NH_2$ groups is in line with the protein concentration in supernatant, R_2 of supernatant is likely to be associated with protein concentration, and even $–NH_2$ concentration. Therefore, associations between the $–NH_2$ group concentration and the average R_2-supernatant during *in vitro* digestion of both 15% and 20% gel were plotted (with $R^2 = 0.91$ for 15% gel and $R^2 = 0.71$ for 20% gel) (Fig. 6). Stronger association for 15% gel is probably due to the faster digestion; more peptide released to the supernatant increases the accuracy of detection. The observed linear relationship demonstrates that the digestion of protein gel, as indicated by the increase of $–NH_2$ group concentration in supernatant, is positively associated with increase of the average R_2 of supernatant. Thus, the average R_2 of supernatant (TD-NMR) can be used to track the *in vitro* digestion of WPI gel, by indicating the amount of protein fraction (the concentration of $–NH_2$ groups) in supernatant.

The relative amplitude of gel fraction (Rel.Ampl.$_{Gel}$) during *in vitro* digestion is shown in Fig. 7a. Under control conditions, the Rel.Ampl.$_{Gel}$ for the 15% gel increased, and that for the 20% gel it slightly decreased in the beginning but then increased to the initial value. In contrast, under digestion conditions the Rel.Ampl.$_{Gel}$ of both 15% and 20% gel decreased over time. Changes in Rel.Ampl.$_{Gel}$ might be caused by two factors: 1) gel structure breakdown, resulting in transferring of protons from solid gel into liquid supernatant, which mainly happens under digestion conditions; and 2) swelling pressure-induced water migration (Flory & Rehner, 1943; Quesada-Pérez, Maroto-Centeno, Forcada, & Hidalgo-Alvarez, 2011; van der Sman, 2015), which results in either swelling or shrinking of the gels (this can take place under both digestion and control conditions).

Therefore, to further elucidate the mechanism, the swelling/shrinking properties were measured (Fig. 7b). The results indicate that with 15% gel there was 5.7% swelling in 120 min, while for 20% gel slight shrinking in the first 30 min and then 1% swelling after 120 min was observed. These different swelling ratios of 15% and 20% gel are thought to be due to the difference in cross-linking density of the gel (de Kruif, Anema, Zhu, Havea, & Coker, 2015). This might confirm the pervious hypothesis on the change of Rel.Ampl.$_{Gel}$ under control conditions: the increase in relative amplitude of 15% gel is due to swelling, which causes a growing water proton population in the gel phase over time. In contrast, the 20% gel first shrank in SGF causing a slight decrease of Rel.Ampl.$_{Gel}$ in the beginning and then swelled back to its original state, coherent with the increase of Rel.Ampl.$_{Gel}$ to its original value. Compared with the control condition, for both 15% and 20% gel, larger decreases of Rel.Ampl.$_{Gel}$ under digestion conditions are due to breakdown of the gel phase. Therefore, to eliminate the effect of swelling/shrinking, ΔRel.Ampl.$_{Gel}$ was calculated by subtracting change of Rel.Ampl.$_{Gel}$ under control condition from that under digestion conditions. An negative linear association between ΔRel.Ampl.$_{Gel}$ and protein concentration in supernatant was observed (Fig. 7c). This demonstrates that there were fewer protons in the gel phase with more protein present in the supernatant over time. Thus, the ΔRel.Ampl.$_{Gel}$ can indicate the breakdown of protein gel during *in vitro* digestion. The swelling/shrinking properties of the gels clearly affect the value of Rel.Ampl.$_{Gel}$. This provides an important avenue for further research. In particular, on the effects of swelling and shrinking on digestion.

3.4. Monitoring gastric digestion with MRI

Next, we used MRI to monitor *in vitro* gastric digestion of protein gels. Fig. 8a shows the color-coded T_2 (MRI) distribution in a cross section of tubes with 15% gel and SGF. Protein gel (lower part of the picture) and supernatant (upper part of the picture) compartments can be distinguished as well as the change in their T_2 spatial distribution over time. Under digestion conditions, the T_2 of supernatant decreased as reflected in the gradual darker color of the supernatant region, with the exception of time points 0–10 min, while under control conditions, there was no change. The decrease of T_2-supernatant during digestion is caused by the increase of protein fraction. The reason that under digestion conditions time points 0–10 min do not follow the above-described trend is because initially the temperature of the SGF with pepsin did not rise up to 37 °C, and this lower temperature induces a shorter T_2 (Mariette, 2009). For 20% gel, under both control and digestion conditions, there was no observable change in the T_2 (MRI) over time (Supplemental Fig. 2). This is caused by the lower degree of digestion compared with the 15% gel. Therefore, further discussion mainly focuses on the 15% gel results.

To make direct comparison with the result of TD-NMR, whole digestion mixtures were segmented and histogram of T_2 distribution in the digestion mixture against the corresponding number of voxels was

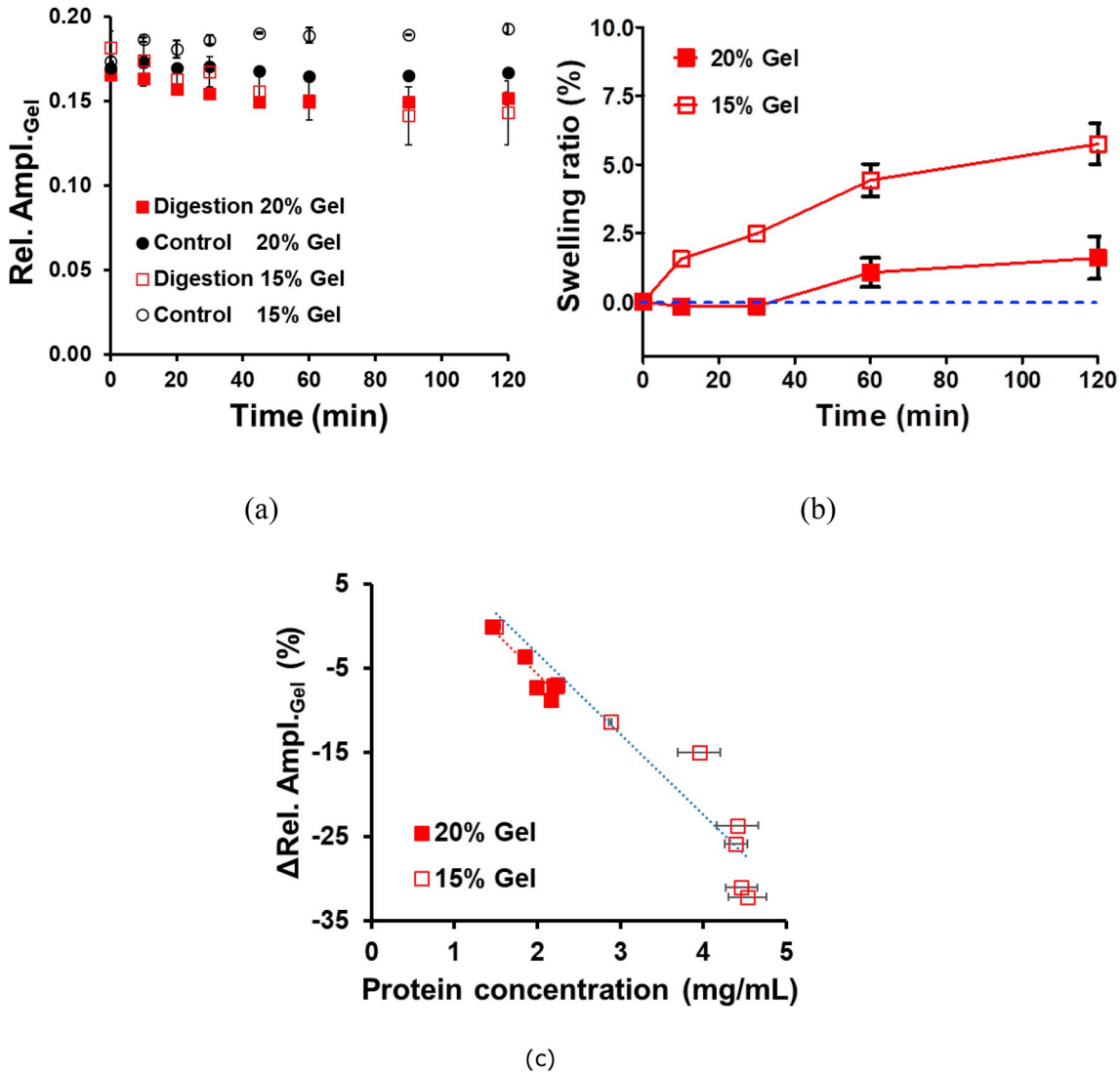

Fig. 7. Relative amplitude of the gel phase (a) and swelling ratio of gel in SGF (without pepsin) (b) over time, and correlation between ΔRel.Ampl.$_{Gel}$ and protein concentration in supernatant of 20% WPI gel (R^2 = 0.85) and 15% WPI gel (R^2 = 0.88) (c) during 120 min of *in vitro* gastric digestion. Error bars are based on the standard deviation of two or three experiments. The calculation for Rel.Ampl.$_{Gel}$ and ΔRel.Ampl.$_{Gel}$ can be found in *2.4*.

obtained. The T_2 distribution of the 15% gel digestion mixture before digestion is shown in Fig. 8b. In the T_2 distribution, the two major peaks with average T_2 values of 337 m s and 1676 m s represent the gel and SGF, respectively. This is comparable with the T_2 (TD-NMR) distribution in Fig. 1b where the gel peak is at 76 m s and the SGF peak at 2400 m s. The separation of the two peaks based on the T_2 (MRI) histogram was less clear than in the TD-NMR data. We hypothesized this may be due to partial volume effects (Angel, Zisserman, & Brady, 2002); since the diameter of gel particles is smaller than the voxel size, one voxel may contain both SGF and gel. As shown in Supplemental Fig. 3., phasor analysis (Vergeldt et al., 2017) was employed and confirmed our hypothesis about the partial volume effect.

Since the separation of gel and SGF/supernatant in the T_2 histogram was less clear, more accurate phase identification was done by regular approach of MRI image analysis (by directly selecting the region of interest (e.g. supernatant phase) manually as described in 2.5). Subsequently, the average T_2-supernatant (MRI) and R_2-supernatant (MRI) were calculated from the supernatant region instead of using the supernatant peak from T_2 (MRI) histogram. Guided by the interpretation of TD-NMR results, R_2-supernatant (MRI) was correlated with the concentration of $-NH_2$ groups in SGF. There was a linear positive correlation, except at time points 0 and 10 min because of the temperature difference (Fig. 9a). Furthermore, ΔFraction$_{Gel}$, representing the change in gel volume due to digestion, correlated negatively with supernatant protein concentration (Fig. 9b). Thus, similar with the results from TD-NMR, not only the average R_2-supernatant (MRI) can be used to monitor hydrolysis of WPI gel by indicating the amount of protein fraction ($-NH_2$ groups concentration) in the supernatant during digestion; but also the volume change of gel can be visualized by T_2-mapping (MRI) to indicate the breakdown of protein gel during digestion.

Future work may focus on further development of the MRI measurement sequence in order to acquire a 3D data set within an acceptable measuring time period (suitable for breath holding). Further, the influence of meal portion, pH, gastric secretion, and gastric emptying on the magnetic resonance parameters should be investigated, so as to lay a solid foundation to link *in vivo* experiments.

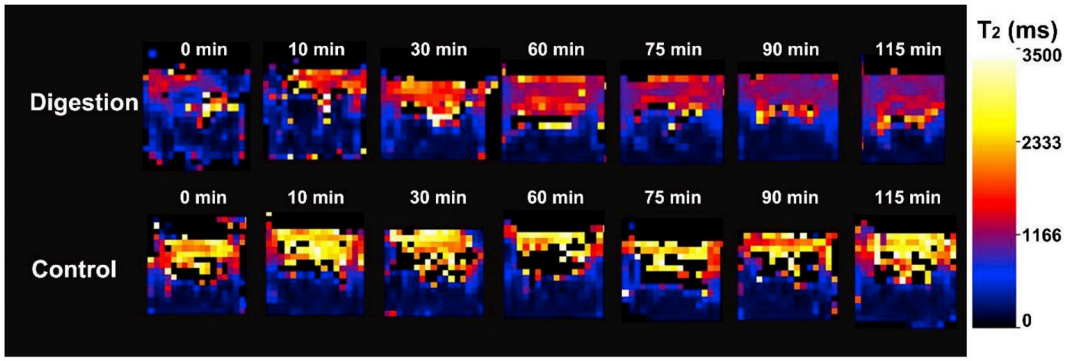

(a)

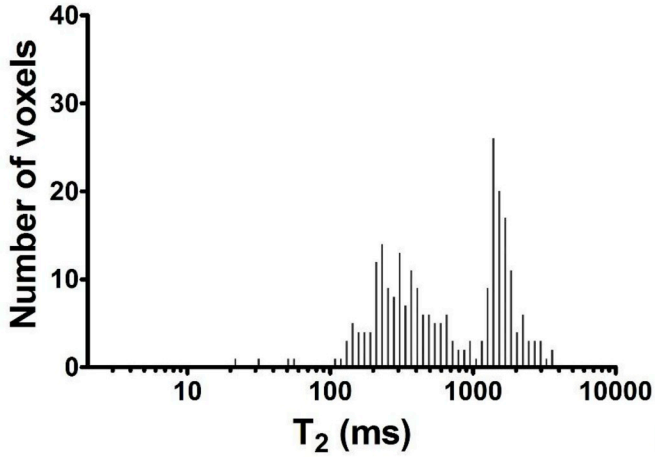

(b)

Fig. 8. Color-coded T_2 (MRI) images (in which each pixel was color-coded according to its T_2 value with light yellow to dark blue representing T_2 value from 3500 m s to 0 m s) of 15% WPI gel under digestion condition (with pepsin) and control condition (without pepsin) from time 0–115 min (a) and T_2 (MRI) distribution of 15% gel at digestion time 0 min (b). (For interpretation of the references to color in this figure legend, the reader is referred to the Web version of this article.)

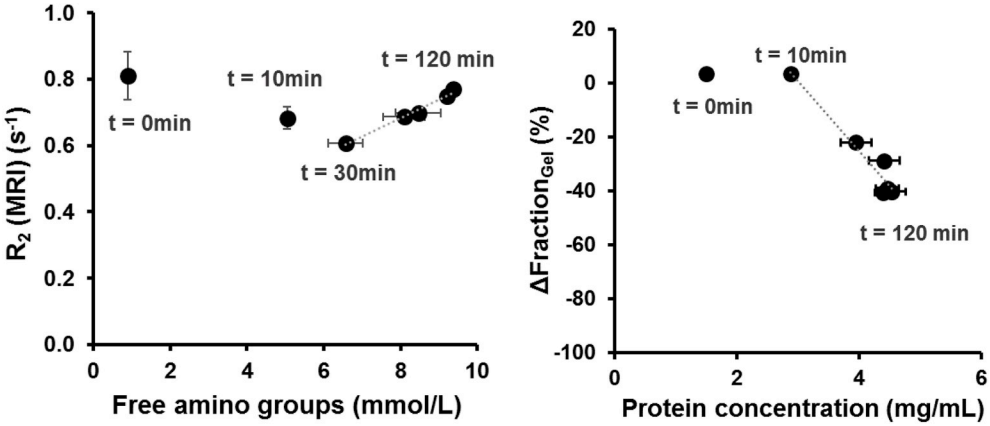

(a) (b)

Fig. 9. Correlation between average R_2 of supernatant (MRI) and free amino groups in the supernatant (R^2 = 0.96) (a) and correlation between $\Delta Fraction_{Gel}$ (MRI) and protein concentration in the supernatant (R^2 = 0.94) (b). Error bars are based on the standard deviation of two or three experiments. The calculation for $\Delta Fraction_{Gel}$ can be found in *2.5*.

Conclusion

To verify the *in vitro* findings on gastric digestion of protein rich food in humans, developing a method that is applicable for both contexts is crucial. Here we proposed MRI as the method. To our knowledge, this study is the first to employ TD-NMR T_2 measurements as a method to monitor protein gel hydrolysis during *in vitro* gastric digestion and to subsequently validate it in an MRI setting. We established that *in vitro* gastric digestion of WPI gel can be monitored by TD-NMR T_2 measurement, including: 1) the R_2 value of supernatant, which is linearly correlated with protein (–NH_2 groups) concentration (a marker of degree of hydrolysis) in supernatant; 2) the relative amplitude of the gel fraction, which reflects the change in proton population due to water migration and gel breakdown. Digestion of WPI gel can be

monitored by MRI T_2-mapping as well, with R_2–supernatant (MRI) and detecting volume change of the gel. Compared to TD-NMR, spatial information in MRI T_2-maps contributed to the phase separation of the fluid and gel fractions. In conclusion, this study shows that MRI has high potential for monitoring *in vivo* gastric digestion and strengthens our ambition of bridging *in vitro* and *in vivo* gastric digestion research with the use of magnetic resonance techniques.

Conflict of interest

The authors declare no conflict of interest.

Acknowledgement

This work was supported by China Scholarship Council. The use of the 3T MRI facility has been made possible by Wageningen University & Research Shared Research Facilities. The authors thank Yusi Ma for assisting the MRI measurement.

Appendix A. Supplementary data

Supplementary data to this article can be found online at https://doi.org/10.1016/j.foodhyd.2019.105348.

References

Angel, M., Zisserman, A. P., & Brady, M. (2002). Estimation of the partial volume effect in. *Magnetic Resonance Imaging, 6*, 389–405.

Bazin, P. L., Cuzzocreo, J. L., Yassa, M. A., Gandler, W., McAuliffe, M. J., Bassett, S. S., et al. (2007). Volumetric neuroimage analysis extensions for the MIPAV software package. *Journal of Neuroscience Methods, 165*(1), 111–121. https://doi.org/10.1016/j.jneumeth.2007.05.024.

Bordoni, A., Laghi, L., Babini, E., Di Nunzio, M., Picone, G., Ciampa, A., et al. (2014). The foodomics approach for the evaluation of protein bioaccessibility in processed meat upon in vitro digestion. *Electrophoresis, 35*(11), 1607–1614. https://doi.org/10.1002/elps.201300579.

Bordoni, A., Picone, G., Babini, E., Vignali, M., Danesi, F., Valli, V., et al. (2011). NMR comparison of in vitro digestion of Parmigiano Reggiano cheese aged 15 and 30 months. *Magnetic Resonance in Chemistry, 49*(SUPPL. 1)https://doi.org/10.1002/mrc.2847.

Bornhorst, G. M., & Paul Singh, R. (2014). Gastric digestion in vivo and in vitro: How the structural aspects of food influence the digestion process. *Annual Review of Food Science and Technology, 5*(1), 111–132. https://doi.org/10.1146/annurev-food-030713-092346.

Bosmans, G. M., Lagrain, B., Deleu, L. J., Fierens, E., Hills, B. P., & Delcour, J. A. (2012). Assignments of proton populations in dough and bread using NMR relaxometry of starch, gluten, and flour model systems. *Journal of Agricultural and Food Chemistry, 60*(21), 5461–5470. https://doi.org/10.1021/jf3008508.

Brodkorb, A., Egger, L., Alminger, M., Alvito, P., Assunção, R., Ballance, S., et al. (2019). INFOGEST static in vitro simulation of gastrointestinal food digestion. *Nature Protocols, 14*(4), 991–1014. https://doi.org/10.1038/s41596-018-0119-1.

Collewet, G., Bugeon, J., Idier, J., Quellec, S., Quittet, B., Cambert, M., et al. (2013). Rapid quantification of muscle fat content and subcutaneous adipose tissue in fish using MRI. *Food Chemistry, 138*(2–3), 2008–2015. https://doi.org/10.1016/j.foodchem.2012.09.131.

Dekkers, B. L., de Kort, D. W., Grabowska, K. J., Tian, B., Van As, H., & van der Goot, A. J. (2016). A combined rheology and time domain NMR approach for determining water distributions in protein blends. *Food Hydrocolloids, 60*, 525–532. https://doi.org/10.1016/j.foodhyd.2016.04.020.

Dinakar, P., & Kilara, A. (1996). Enhancing the functionality of food proteins by enzymatic modification. *Trends in Food Science & Technology, 7*(4), 120–125. Retrieved from https://doi.org/10.1016/0924-2244(96)10012-1.

van Duynhoven, J., Voda, A., Witek, M., & Van As, H. (2010). (1st ed.). *Time-domain NMR applied to food products. Annual Reports on NMR SpectroscopyVol. 69*Elsevier Ltdhttps://doi.org/10.1016/S0066-4103(10)69003-5.

Flory, P. J., & Rehner, J. (1943). Statistical mechanics of cross-linked polymer networks II. Swelling. *The Journal of Chemical Physics, 11*(11), 521–526. https://doi.org/10.1063/1.1723792.

Hills, B. P., Takacs, S. F., & Belton, P. S. (1990). A new interpretation of proton NMR relaxation time measurements of water in food. *Food Chemistry, 37*(2), 95–111. https://doi.org/10.1016/0308-8146(90)90084-H.

Kirtil, E., Cikrikci, S., McCarthy, M. J., & Oztop, M. H. (2017). Recent advances in time domain NMR & MRI sensors and their food applications. *Current Opinion in Food Science, 17*, 9–15. https://doi.org/10.1016/j.cofs.2017.07.005.

Kong, F., & Singh, R. P. (2008). A model stomach system to investigate disintegration kinetics of solid foods during gastric digestion. *Journal of Food Science, 73*(5), 202–210. https://doi.org/10.1111/j.1750-3841.2008.00745.x.

de Kruif, C. G.(K.)., Anema, S. G., Zhu, C., Havea, P., & Coker, C. (2015). Water holding capacity and swelling of casein hydrogels. *Food Hydrocolloids, 44*, 372–379. https://doi.org/10.1016/j.foodhyd.2014.10.007.

Lavenson, D. M., Tozzi, E. J., McCarthy, M. J., Powell, R. L., & Jeoh, T. (2011). Investigating adsorption of bovine serum albumin on cellulosic substrates using magnetic resonance imaging. *Cellulose, 18*(6), 1543–1554. https://doi.org/10.1007/s10570-011-9588-x.

Le Dean, A., Mariette, F., & Marin, M. (2004). 1H nuclear magnetic resonance relaxometry study of water state in milk protein mixtures. *Journal of Agricultural and Food Chemistry, 52*(17), 5449–5455. https://doi.org/10.1021/jf030777m.

Li, M., Li, B., & Zhang, W. (2018). Rapid and non-invasive detection and imaging of the hydrocolloid-injected prawns with low-field NMR and MRI. *Food Chemistry, 242*(August 2017), 16–21. https://doi.org/10.1016/j.foodchem.2017.08.086.

Luo, Q., Boom, R. M., & Janssen, A. E. M. (2015). Digestion of protein and protein gels in simulated gastric environment. *Lebensmittel-Wissenschaft und -Technologie- Food Science and Technology, 63*(1), 161–168. https://doi.org/10.1016/j.lwt.2015.03.087.

Luo, Q., Borst, J. W., Westphal, A. H., Boom, R. M., & Janssen, A. E. M. (2017). Pepsin diffusivity in whey protein gels and its effect on gastric digestion. *Food Hydrocolloids, 66*, 318–325. https://doi.org/10.1016/j.foodhyd.2016.11.046.

Maclerzanka, A., Böttger, F., Lansonneur, L., Groizard, R., Jean, A. S., Rigby, N. M., et al. (2012). The effect of gel structure on the kinetics of simulated gastrointestinal digestion of bovine β-lactoglobulin. *Food Chemistry, 134*(4), 2156–2163. https://doi.org/10.1016/j.foodchem.2012.04.018.

Marciani, L. (2011). Assessment of gastrointestinal motor functions by MRI: A comprehensive review. *Neuro-Gastroenterology and Motility, 23*(5), 399–407. https://doi.org/10.1111/j.1365-2982.2011.01670.x.

Marciani, L., Manoj, P., Hills, B. P., Moore, R. J., Young, P., Fillery-Travis, A., et al. (1998). Echo-planar imaging relaxometry to measure the viscosity of a model meal. *Journal of Magnetic Resonance, 135*(1), 82–86. https://doi.org/10.1006/jmre.1998.1560.

Mariette, F. (2009). Investigations of food colloids by NMR and MRI. *Current Opinion in Colloid & Interface Science, 14*(3), 203–211. https://doi.org/10.1016/j.cocis.2008.10.006.

Messroghli, D. R., Rudolph, A., Abdel-Aty, H., Wassmuth, R., Kuhne, T., Dietz, R., et al. (2010). An open-source software tool for the generation of relaxation time maps in magnetic resonance imaging. *BMC Medical Imaging, 10*, 16. https://doi.org/10.1186/1471-2342-10-16.

Minekus, M., Alminger, M., Alvito, P., Ballance, S., Bohn, T., Bourlieu, C., et al. (2014). A standardised static in vitro digestion method suitable for food-an international consensus. *Food and Function, 5*(6), 1113–1124. https://doi.org/10.1039/c3fo60702j.

Munialo, C. D., van der Linden, E., Ako, K., Nieuwland, M., Van As, H., & de Jongh, H. H. J. (2016). The effect of polysaccharides on the ability of whey protein gels to either store or dissipate energy upon mechanical deformation. *Food Hydrocolloids, 52*, 707–720. https://doi.org/10.1016/j.foodhyd.2015.08.013.

Nott, K. P., & Hall, L. D. (2005). Validation and cross-comparison of MRI temperature mapping against fibre optic thermometry for microwave heating of foods. *International Journal of Food Science and Technology, 40*(7), 723–730. https://doi.org/10.1111/j.1365-2621.2005.00992.x.

Nyemb-Diop, K., Causeur, D., Jardin, J., Briard-Bion, V., Guérin-Dubiard, C., Rutherfurd, S. M., et al. (2016). Investigating the impact of egg white gel structure on peptide kinetics profile during in vitro digestion. *Food Research International, 88*(Part B), 302–309. https://doi.org/10.1016/j.foodres.2016.01.004.

Nyemb, K., Guérin-Dubiard, C., Pézennec, S., Jardin, J., Briard-Bion, V., Cauty, C., et al. (2016). The structural properties of egg white gels impact the extent of in vitro protein digestion and the nature of peptides generated. *Food Hydrocolloids, 54*, 315–327. https://doi.org/10.1016/j.foodhyd.2015.10.011.

Peters, J. P. C. M., Vergeldt, F. J., Van As, H., Luyten, H., Boom, R. M., & van der Goot, A. J. (2016). Time domain nuclear magnetic resonance as a method to determine and characterize the water-binding capacity of whey protein microparticles. *Food Hydrocolloids, 54*, 170–178. https://doi.org/10.1016/j.foodhyd.2015.09.031.

Provencher, S. W., & Vogel, R. H. (1983). In P. Deuflhard, (Ed.). *Numerical treatment of inverse problems in differential and integral equations © birkhäuser* (pp. 304–305). Boston 1983.

Quesada-Pérez, M., Maroto-Centeno, J. A., Forcada, J., & Hidalgo-Alvarez, R. (2011). Gel swelling theories: The classical formalism and recent approaches. *Soft Matter, 7*(22), 10536–10547. https://doi.org/10.1039/c1sm06031g.

Schmidt, D. G., Meijer, R. J. G. M., Slangen, C. J., & Van Beresteijn, E. C. H. (1995). Raising the pH of the pepsin-catalysed hydrolysis of bovine whey proteins increases the antigenicity of the hydrolysates. *Clinical and Experimental Allergy, 25*(10), 1007–1017. https://doi.org/10.1111/j.1365-2222.1995.tb00404.x.

Singh, H., & Gallier, S. (2014). Processing of food structures in the gastrointestinal tract and physiological responses. *Food Structures, Digestion and Health*. https://doi.org/10.1016/B978-0-12-404610-8.00002-5.

Singh, H., Ye, A., & Ferrua, M. J. (2015). Aspects of food structures in the digestive tract. *Current Opinion in Food Science, 3*, 85–93. https://doi.org/10.1016/j.cofs.2015.06.007.

van der Sman, R. G. M. (2015). Biopolymer gel swelling analysed with scaling laws and Flory-Rehner theory. *Food Hydrocolloids, 48*, 94–101. https://doi.org/10.1016/j.foodhyd.2015.01.025.

Spiller, R., & Marciani, L. (2019). Intraluminal impact of food: New insights from MRI. *Nutrients, 11*(5), 1147. https://doi.org/10.3390/nu11051147.

Vergeldt, F. J., Prusova, A., Fereidouni, F., Van Amerongen, H., Van As, H., Scheenen, T. W. J., et al. (2017). Multi-component quantitative magnetic resonance imaging by phasor representation. *Scientific Reports, 7*(1), 1–10. https://doi.org/10.1038/s41598-017-00864-8.